

STRUCTURAL AND ECOTOXICOLOGICAL PROFILE OF N-ALKOXYMORPHOLINIUM-BASED IONIC LIQUIDS

**Robert Salchner,¹ Gerhard Laus,¹ Simone Haslinger,¹ Volker
Kahlenberg,² Klaus Wurst,¹ Doris E. Braun,¹ Stefan Vergeiner,¹
Holger Kopacka,¹ Herwig Schottenberger,^{1*} Alan Puckowski,^{3,4}
Marta Markiewicz,³ Stefan Stolte,^{3,4} Sven Nerdinger^{5*}**

¹ Faculty of Chemistry and Pharmacy, Leopold-Franzens University, Innrain 80, 6020 Innsbruck, Austria. ² Institute of Mineralogy and Petrography, Leopold-Franzens University, Innrain 52, 6020 Innsbruck. ³ Department of Environmental Analysis, Institute of Environmental Protection and Human Health, Faculty of Chemistry, University of Gdańsk, ul. Wita Stwosza 63, 80-308 Gdańsk, Poland. ⁴ UFT - Center for Environmental Research and Sustainable Technology, University of Bremen, Leobener Strasse, 28359 Bremen, Germany. ⁵ Sandoz GmbH, Biochemiestrasse 10, 6250 Kundl, Austria.

Supporting Information

Contents

X-ray powder diffraction patterns and Pawley fits

Hydrogen interaction geometries

Temperature dependence of dynamic viscosity η of compounds **12**, **13**, **16**, and **17**

¹H and ¹³C NMR of paramagnetic tetrachloroferrates(III) **4** and **5**

Acetylcholinesterase inhibition assay

Cell viability assay with IPC-81 cells

Reproduction inhibition assay with limnic green algae *Scenedesmus vacuolatus*

Statistical analysis

Primary biodegradation

X-ray powder diffraction. XRPD patterns were obtained using a X'Pert PRO diffractometer (PANalytical, Almelo, NL) equipped with a theta/theta coupled goniometer in transmission geometry, programmable XYZ stage with well plate holder, $\text{CuK}\alpha_{1,2}$ radiation source with a focussing mirror, a 0.5° divergence slit and a 0.02° Soller slit collimator on the incident beam side, a 2 mm antiscattering slit and a 0.02° Soller slit collimator on the diffracted beam side and a solid state PIXcel detector. The patterns were recorded at a tube voltage of 40 kV, tube current of 40 mA, applying a step size of $2\theta = 0.007^\circ$ with 80s per step in the 2θ range between 2° and 40° .

Pawley-Fit. Pawley fits were performed with Topas Academic V5 (Topas Academic V5, Coelho Software, Brisbane, 2012). The background was modelled with Chebyshev polynomials and the modified Thompson-Cox-Hastings pseudo-Voigt (TCHZ) function was used for peak shape fitting.

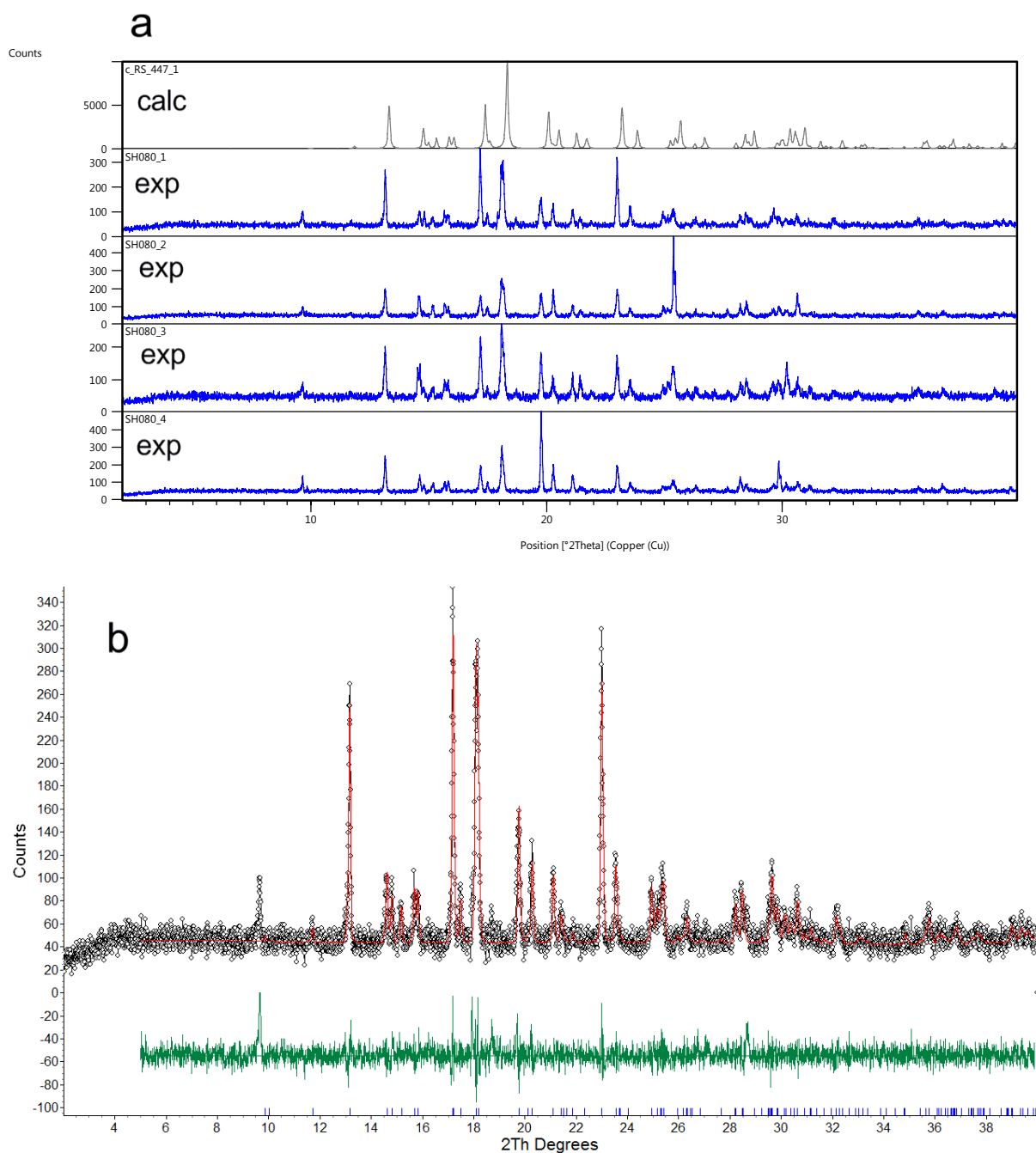


Figure S1. (a) Calculated and experimental PXR D patterns of *N*-methoxy-*N*-methylmorpholinium tetrachloroferrate (**4**), (b) Pawley fit ($R_{wp} = 12.86$, $R_{exp} = 13.49$, $R_p = 9.90$, $gof = 0.95$) between the reflection PXR D data with a model consisting of the cell parameters derived from the single crystal structure. Black dots indicate raw data, while the red line indicates the calculated model. Tick marks (blue) are the 2θ positions for the hkl reflections. The difference pattern is shown in green.

Table S1. Comparison of lattice parameters determined at 133 K (single crystal X-ray diffraction data) and 298 K (powder X-ray diffraction data).

4	Space group	$a / \text{\AA}$	$b / \text{\AA}$	$c / \text{\AA}$	$\beta / ^\circ$
SCXRD, 133(2) K	$P2_1/c$	7.4690(2)	10.0649(3)	17.7066(5)	94.001(3)
PXR D, 298 K	$P2_1/c$	7.5686(10)	10.1301(28)	17.9946(28)	93.8218(8)

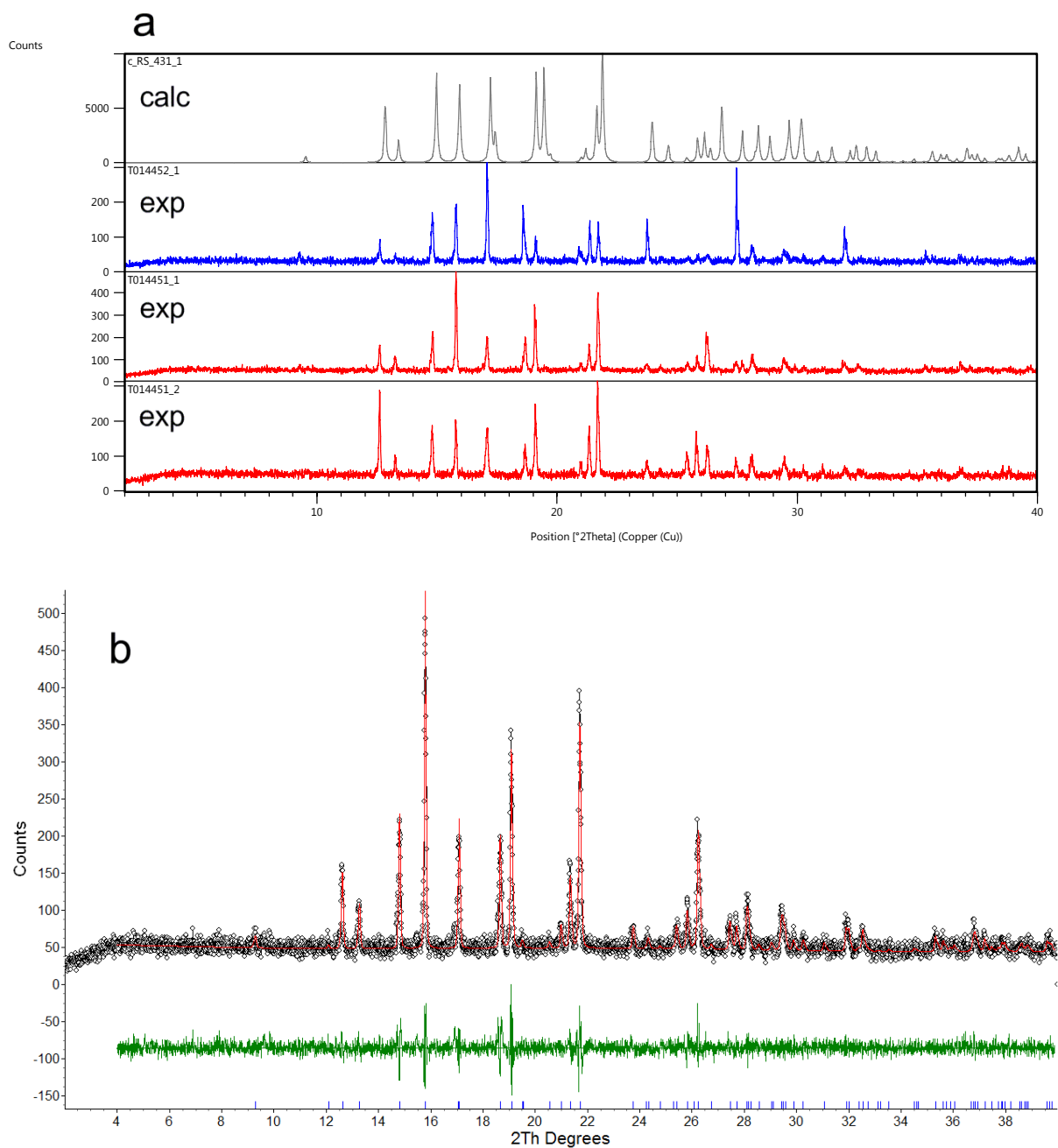


Figure S2. (a) Calculated and experimental PXRD patterns of *N*-ethoxy-*N*-methylmorpholinium tetrachloroferrate (**5**), (b) Pawley fit ($R_{wp} = 12.13$, $R_{exp} = 13.08$, $R_p = 9.61$, $gof = 0.93$) between the reflection PXRD data with a model consisting of the cell parameters derived from the single crystal structure. Black dots indicate raw data, while the red line indicates the calculated model. Tick marks (blue) are the 2θ positions for the hkl reflections. The difference pattern is shown in green.

Table S2. Comparison of lattice parameters determined at 133 K (single crystal X-ray diffraction data) and 298 K (powder X-ray diffraction data).

5	Space group	$a / \text{\AA}$	$b / \text{\AA}$	$c / \text{\AA}$	$\beta / ^\circ$
SCXRD, 133(2) K	$P2_1$	7.4820(3)	10.2834(4)	9.6073(5)	105.257(5)
PXRD, 298 K	$P2_1$	7.5550(8)	10.3623(9)	9.8168(9)	104.610(4)

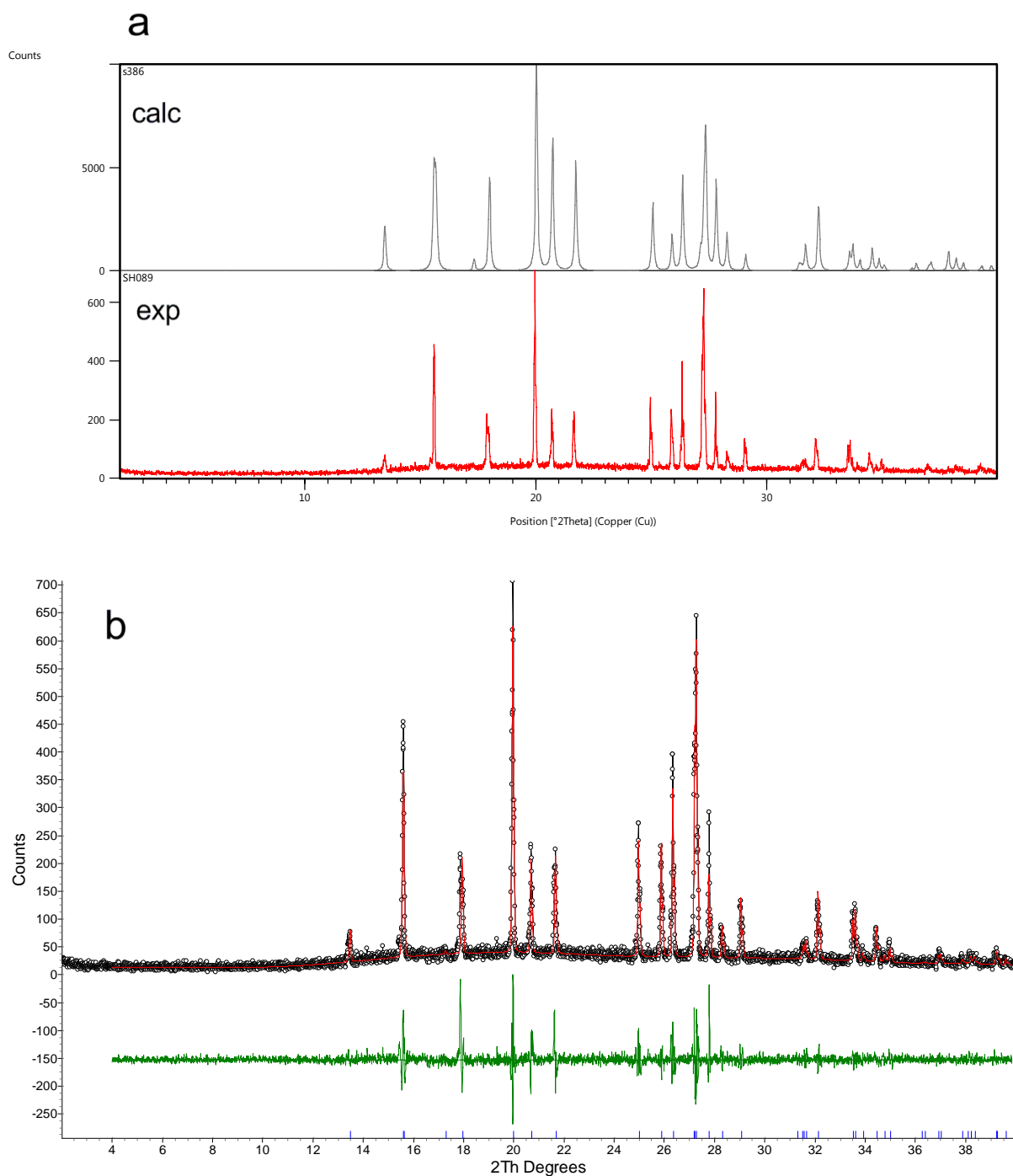


Figure S3. (a) Calculated and experimental PXRD patterns of *N*-methoxy-*N*-methylmorpholinium chloride (**6**), (b) Pawley fit ($R_{wp} = 18.50$, $R_{exp} = 16.27$, $R_p = 14.28$, $gof = 1.14$) between the reflection PXRD data with a model consisting of the cell parameters derived from the single crystal structure. Black dots indicate raw data, while the red line indicates the calculated model. Tick marks (blue) are the 2θ positions for the hkl reflections. The difference pattern is shown in green..

Table S3. Comparison of lattice parameters determined at 233 K (single crystal X-ray diffraction data) and 298 K (powder X-ray diffraction data).

6	Space group	$a / \text{\AA}$	$b / \text{\AA}$	$c / \text{\AA}$	$\beta / ^\circ$
SCXRD, 233(2) K	<i>Cc</i>	5.6130(3)	13.1310(3)	11.4215(6)	98.773(2)
PXRD, 298 K	<i>Cc</i>	5.6311(4)	13.1125(8)	11.4625(7)	98.749(2)

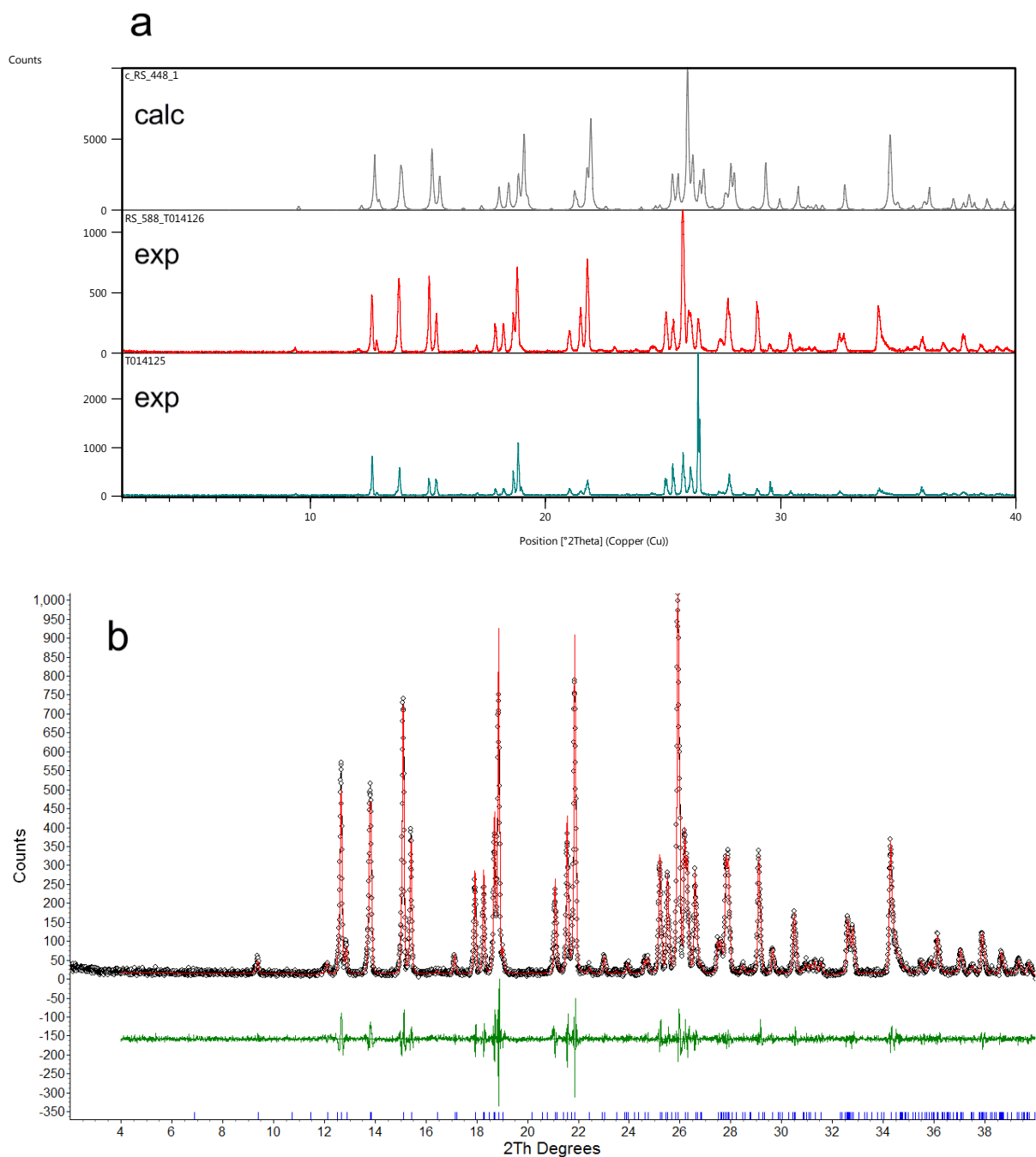


Figure S4. (a) Calculated and experimental PXRD patterns of *N*-ethoxy-*N*-methylmorpholinium chloride hydrate ($7 \cdot \text{H}_2\text{O}$), (b) Pawley fit ($R_{\text{wp}} = 14.37$, $R_{\text{exp}} = 13.71$, $R_{\text{p}} = 10.33$, $\text{gof} = 1.05$) between the reflection PXRD data with a model consisting of the cell parameters derived from the single crystal structure. Black dots indicate raw data, while the red line indicates the calculated model. Tick marks (blue) are the 2θ positions for the hkl reflections. The difference pattern is shown in green..

Table S4. Comparison of lattice parameters determined at 133 K (single crystal X-ray diffraction data) and 298 K (powder X-ray diffraction data).

$7 \cdot \text{H}_2\text{O}$	SG	$a / \text{\AA}$	$b / \text{\AA}$	$c / \text{\AA}$	$\alpha / ^\circ$	$\beta / ^\circ$	$\gamma / ^\circ$
SCXRD, 133(2) K	$P\bar{1}$	8.2618(8)	10.0862(8)	13.0944(12)	78.494(7)	81.588(8)	68.908(8)
PXRD, 298 K	$P\bar{1}$	8.2922(3)	10.1920(4)	13.1237(5)	78.453(2)	81.576(2)	69.074(2)

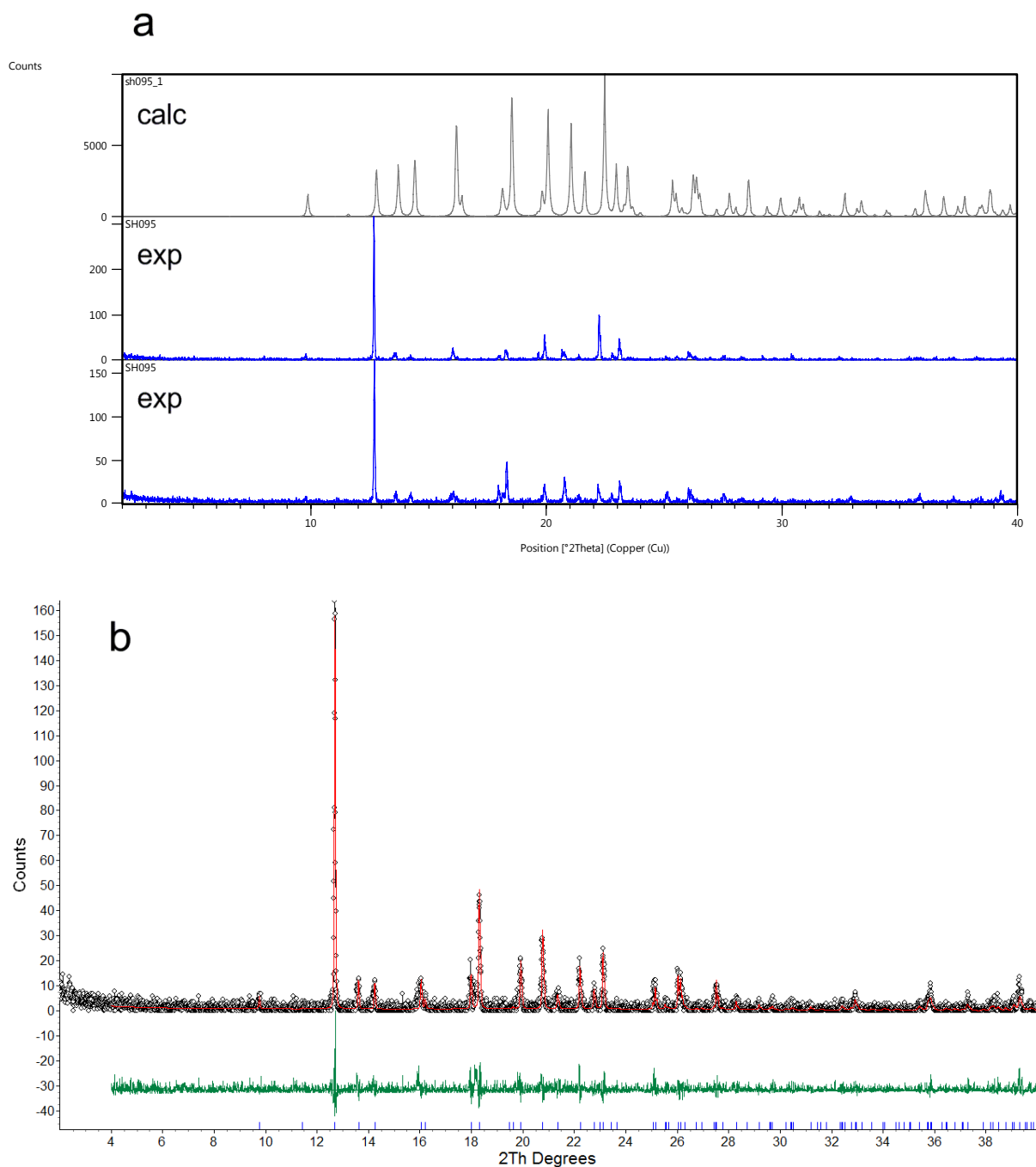


Figure S5. (a) Calculated and experimental PXRD patterns of *N*-methoxy-*N*-methylmorpholinium periodate (**8**), (b) Pawley fit ($R_{wp} = 52.92$, $R_{exp} = 67.18$, $R_p = 45.82$, $gof = 0.79$) between the reflection PXRD data with a model consisting of the cell parameters derived from the single crystal structure. Black dots indicate raw data, while the red line indicates the calculated model. Tick marks (blue) are the 2θ positions for the hkl reflections. The difference pattern is shown in green. Note that the sample liquefied on grinding and the PXRD measurement at 298 K. Therefore, a shorter exposure time of 40s per step, instead of 80s, was chosen, leading to very low peak intensities.

Table S5. Comparison of lattice parameters determined at 173 K (single crystal X-ray diffraction data) and 298 K (powder X-ray diffraction data).

8	Space group	$a / \text{\AA}$	$b / \text{\AA}$	$c / \text{\AA}$	$\beta / ^\circ$
SCXRD, 173(2) K	$P2_1/c$	6.9543(3)	17.8954(7)	8.4838(3)	96.249(4)
PXRD, 298 K	$P2_1/c$	7.0103(8)	18.0867(22)	8.6016(7)	96.615(5)

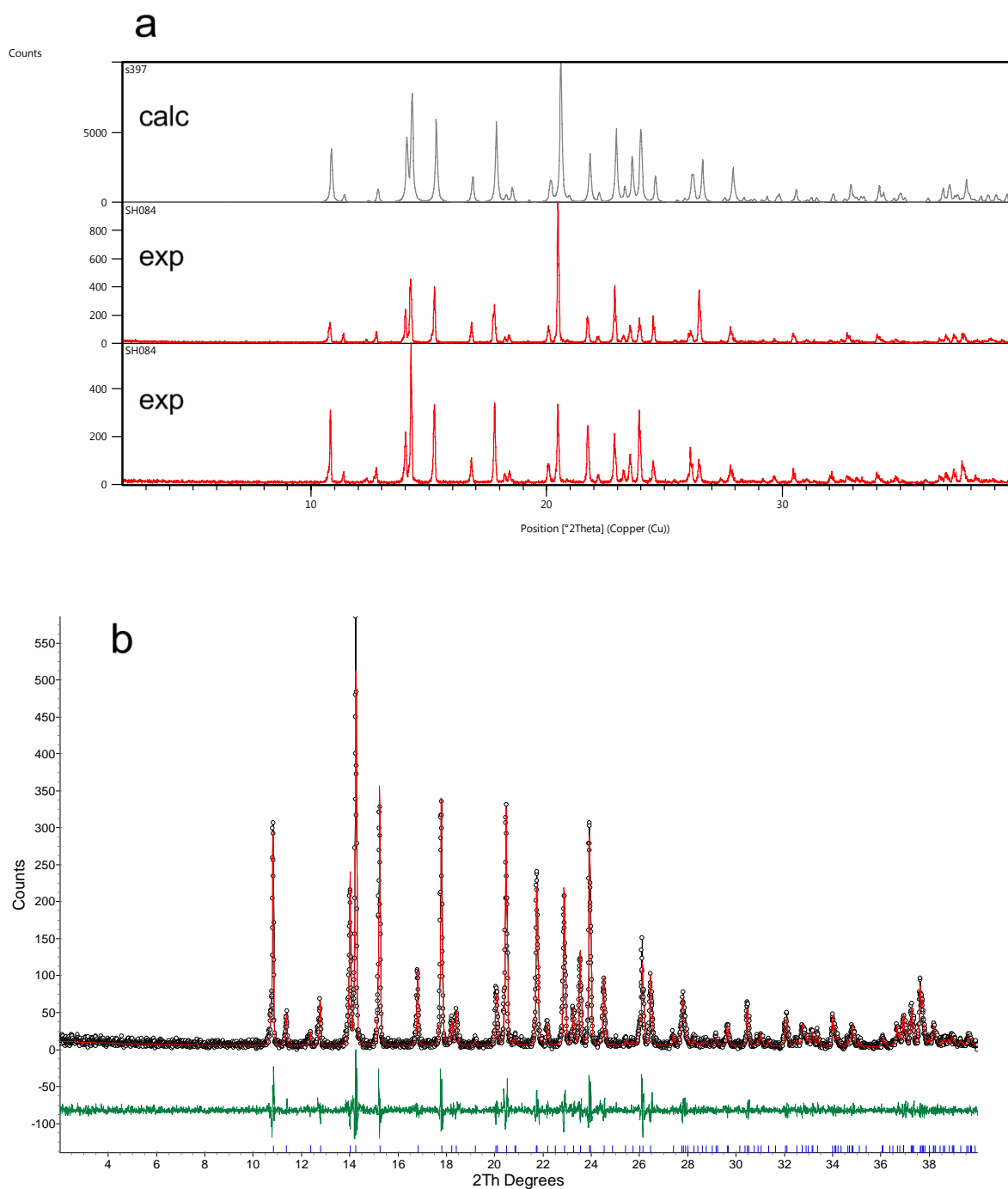


Figure S6. (a) Calculated and experimental PXR D patterns of *N*-ethoxy-*N*-methylmorpholinium periodate (**9**), (b) Pawley fit ($R_{wp} = 23.44$, $R_{exp} = 22.88$, $R_p = 16.84$, $gof = 1.02$) between the reflection PXR D data with a model consisting of the cell parameters derived from the single crystal structure. Black dots indicate raw data, while the red line indicates the calculated model. Tick marks (blue) are the 2θ positions for the hkl reflections. The difference pattern is shown in green.

Table S6. Comparison of lattice parameters determined at 233 K (single crystal X-ray diffraction data) and 298 K (powder X-ray diffraction data).

9	Space group	$a / \text{\AA}$	$b / \text{\AA}$	$c / \text{\AA}$	$\beta / ^\circ$
SCXRD, 233(2) K	$P2_1/n$	9.6497(2)	9.9159(2)	12.4990(3)	97.916(1)
PXR D, 298 K	$P2_1/n$	9.7146(4)	9.9577(4)	12.5279(5)	97.795(3)

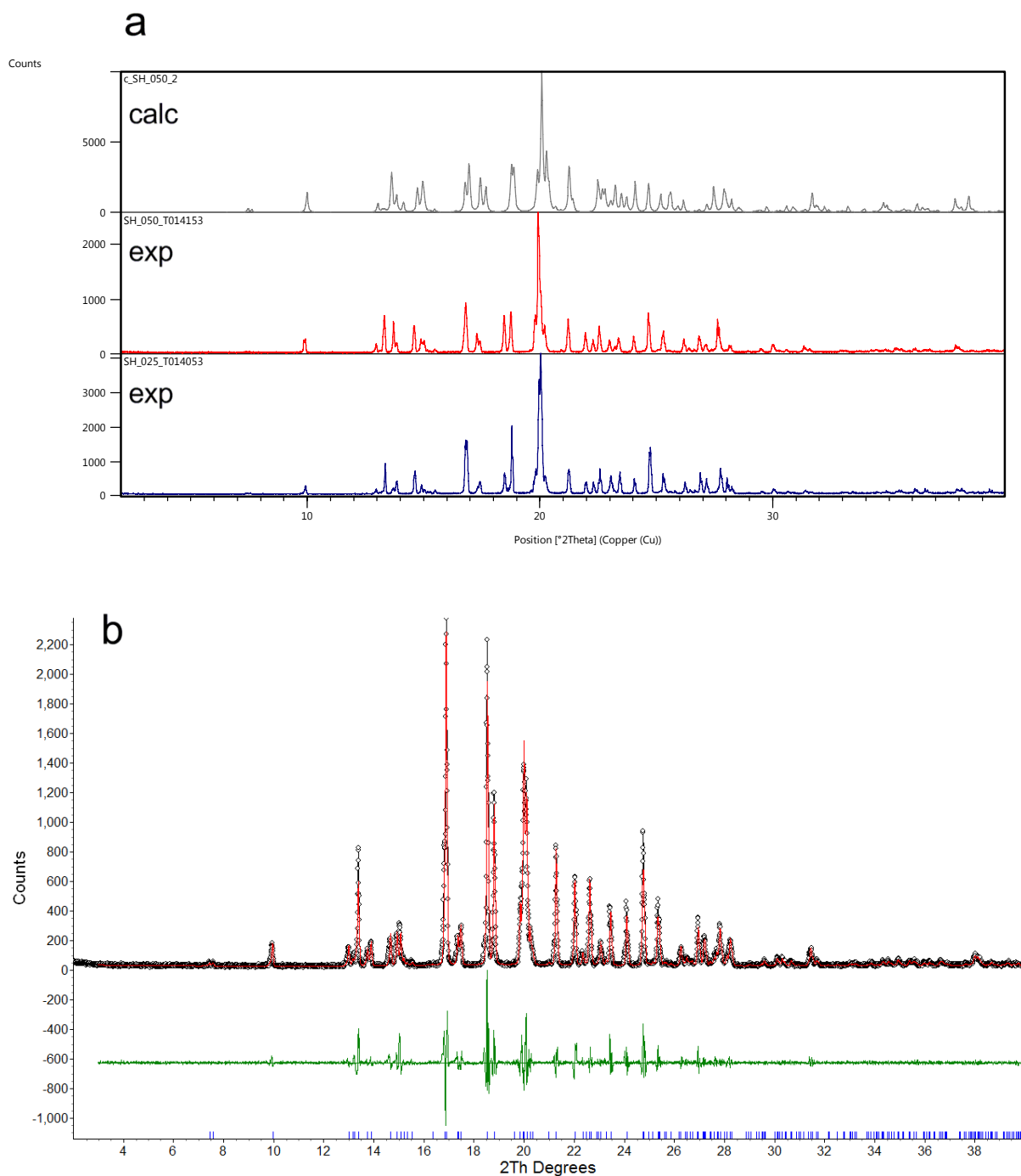


Figure S7. (a) Calculated and experimental PXRD patterns of *N*-ethoxy-*N*-methylmorpholinium tetrafluoroborate (**10**), (b) Pawley fit ($R_{wp} = 18.29$, $R_{exp} = 10.83$, $R_p = 14.26$, $gof = 1.69$) between the reflection PXRD data with a model consisting of the cell parameters derived from the single crystal structure. Black dots indicate raw data, while the red line indicates the calculated model. Tick marks (blue) are the 2θ positions for the hkl reflections. The difference pattern is shown in green.

Table S7. Comparison of lattice parameters determined at 173 K (single crystal X-ray diffraction data) and 298 K (powder X-ray diffraction data).

10	Space group	$a / \text{\AA}$	$b / \text{\AA}$	$c / \text{\AA}$	$\beta / ^\circ$
SCXRD, 173(2) K	$P2_1/n$	7.0137(3)	23.6649(10)	13.3630(6)	96.713(4)
PXRD, 298 K	$P2_1/n$	7.0821(4)	23.7109(13)	13.5146(8)	98.232(3)

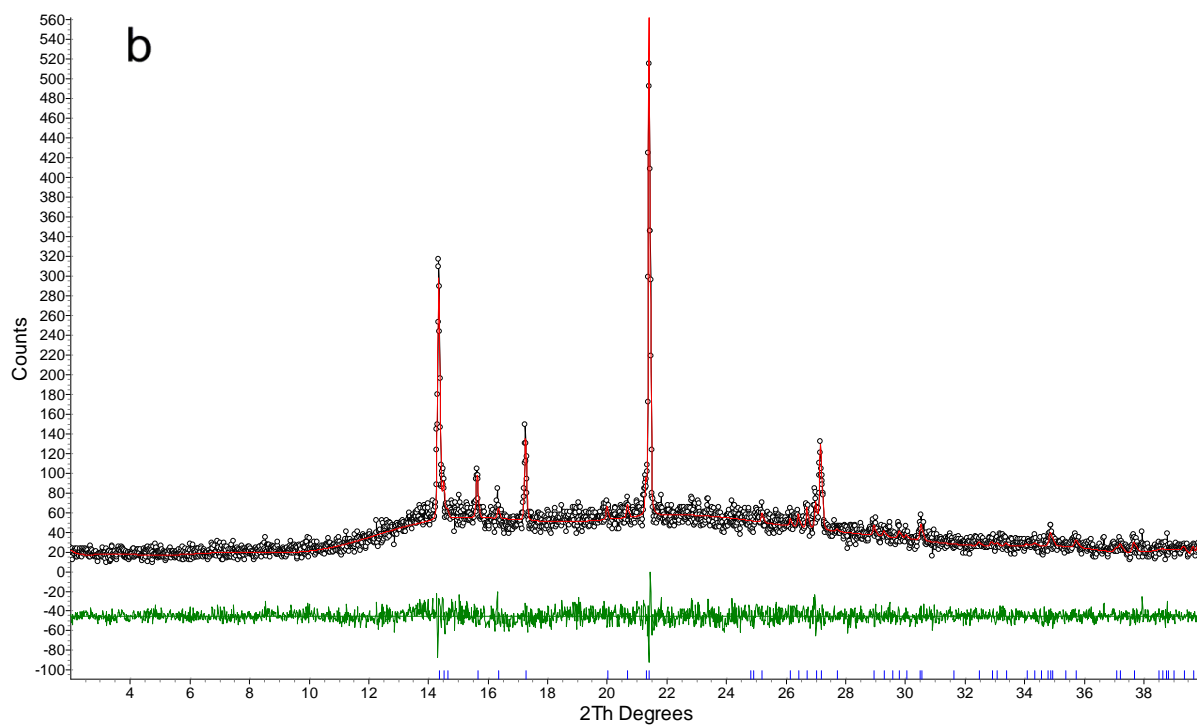
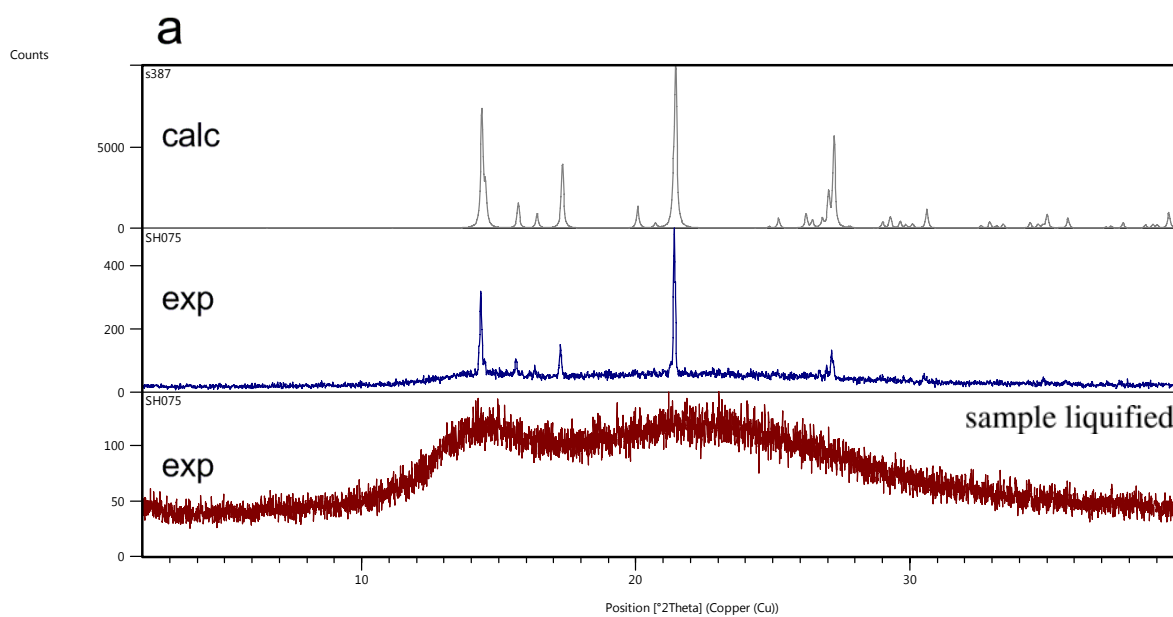


Figure S8. (a) Calculated and experimental PXR patterns of *N*-ethoxy-*N*-methylmorpholinium azide (**11**), (b) Pawley fit ($R_{wp} = 14.21$, $R_{exp} = 15.74$, $R_p = 10.89$, $g_{of} = 0.90$) between the reflection PXR data with a model consisting of the cell parameters derived from the single crystal structure. Black dots indicate raw data, while the red line indicates the calculated model. Tick marks (blue) are the 2θ positions for the hkl reflections. The difference pattern is shown in green.

Table S8. Comparison of lattice parameters determined at 233 K (single crystal X-ray diffraction data) and 298 K (powder X-ray diffraction data).

11	Space group	$a / \text{\AA}$	$b / \text{\AA}$	$c / \text{\AA}$
SCXRD, 233(2) K	$Pna2_1$	11.264(1)	7.122(1)	12.184(1)
PXR, 298 K	$Pna2_1$	11.311(2)	7.142(1)	12.185(2)

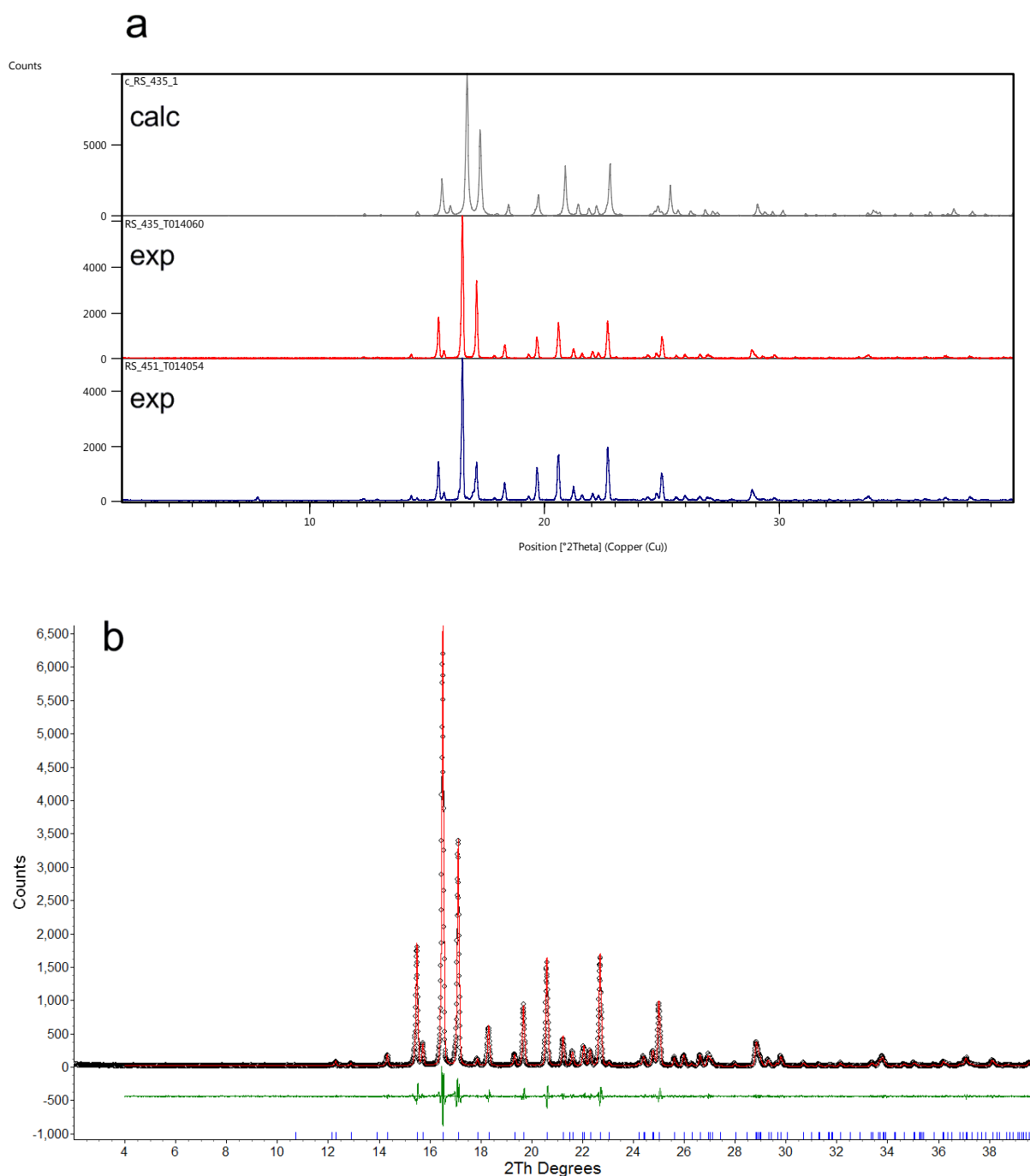


Figure S9. (a) Calculated and experimental PXRD patterns of *N*-ethoxy-*N*-methylmorpholinium hexafluorophosphate (**14**), (b) Pawley fit ($R_{wp} = 11.98$, $R_{exp} = 10.44$, $R_p = 8.95$, $gof = 1.15$) between the reflection PXRD data with a model consisting of the cell parameters derived from the single crystal structure. Black dots indicate raw data, while the red line indicates the calculated model. Tick marks (blue) are the 2θ positions for the hkl reflections. The difference pattern is shown in green.

Table S9. Comparison of lattice parameters determined at 133 K (single crystal X-ray diffraction data) and 298 K (powder X-ray diffraction data).

14	Space group	$a / \text{\AA}$	$b / \text{\AA}$	$c / \text{\AA}$	$\beta / ^\circ$
SCXRD, 133(2) K	$P2_1/n$	8.6207(2)	13.5766(3)	10.4119(2)	99.697(2)
PXRD, 298 K	$P2_1/n$	8.7136(3)	13.6964(5)	10.4660(4)	98.822(1)

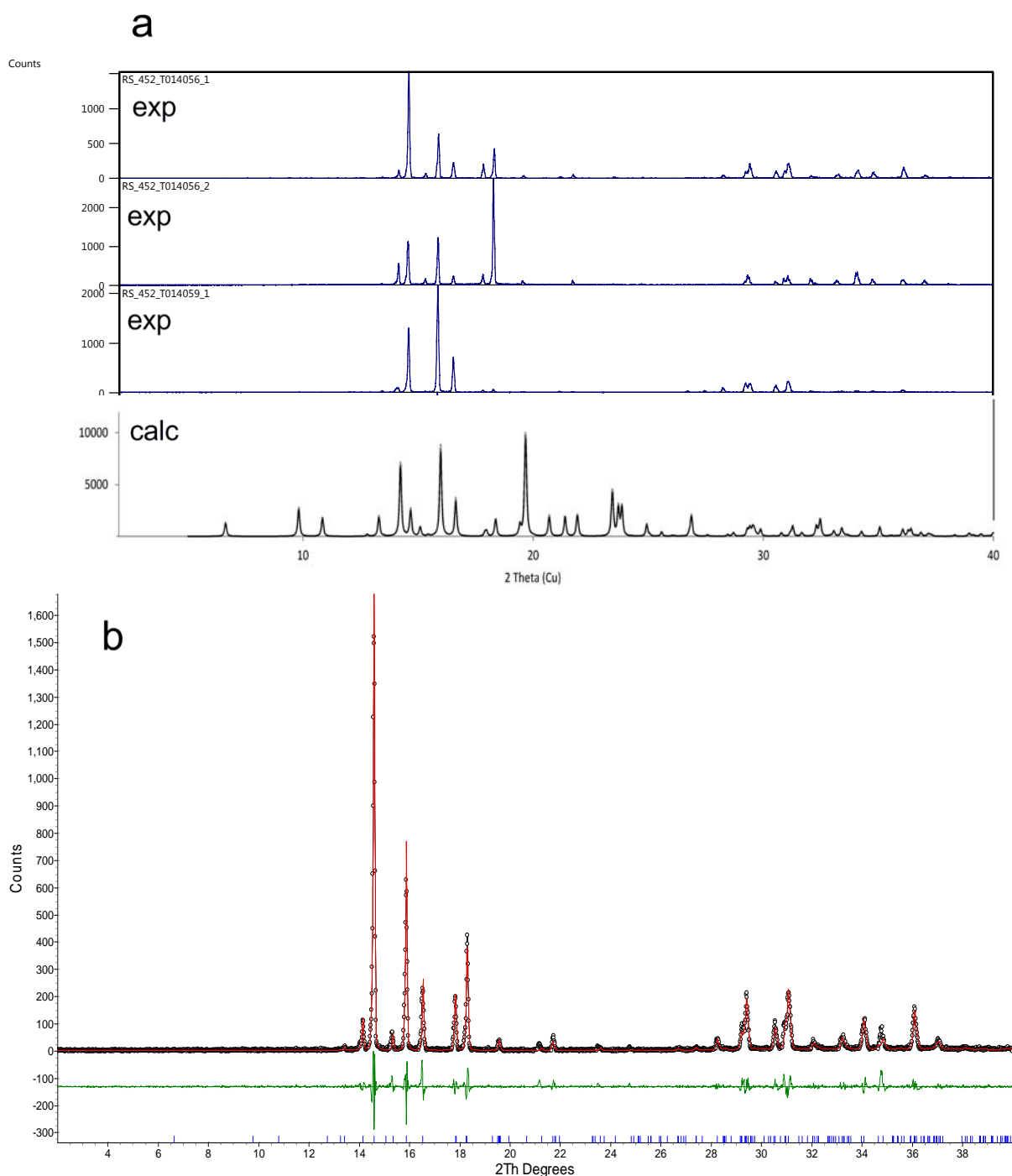


Figure S10. (a) Calculated and experimental PXRD patterns of *N*-ethoxy-*N*-methylmorpholinium triflimide (**15**), (b) Pawley fit ($R_{wp} = 27.47$, $R_{exp} = 22.50$, $R_p = 19.57$, $gof = 1.22$) between the reflection PXRD data with a model consisting of the cell parameters derived from the single crystal structure. Black dots indicate raw data, while the red line indicates the calculated model. Tick marks (blue) are the 2θ positions for the hkl reflections. The difference pattern is shown in green.

Table S10. Comparison of lattice parameters determined at 173 K (single crystal X-ray diffraction data) and 298 K (powder X-ray diffraction data).

15	Space group	$a / \text{\AA}$	$b / \text{\AA}$	$c / \text{\AA}$	$\beta / ^\circ$
SCXRD, 173(2) K	$P2_1/c$	13.5133(4)	7.0313(3)	18.2883(8)	100.108(3)
PXRD, 298 K	$P2_1/c$	13.5497(18)	7.0878(8)	18.3911(26)	100.018(10)

Table S11. Hydrogen interaction geometries (Å, °).

Compound	Interaction	H...A	D...A	D-H...A	Symmetry operation A
4	C5-H...C11	2.7645(6)	3.699(3)	159.5(1)	2-x,1/2+y,1.5-z
	C4-H...C13	2.7888(6)	3.767(2)	170.2(1)	1-x,1/2+y,1.5-z
	C6-H...C12	2.8065(6)	3.786(3)	179.2(2)	1-x,-y,2-z
	C2-H...C12	2.8122(5)	3.727(2)	154.1(1)	2-x,-y,2-z
	C5-H...C14	2.8411(7)	3.793(2)	164.2(1)	x,1+y,z
	C4-H...C12	2.8797(6)	3.813(2)	157.6(1)	x,y,z
	C3-H...O1	2.661(2)	3.138(3)	109.8(1)	2-x,1/2+y,1.5-z
5	C3-H...C11	2.737(1)	3.590(4)	144.7(2)	1-x,1/2+y,-z
	C5-H...C13	2.752(1)	3.703(5)	163.9(2)	1-x,1/2+y,-z
	C5-H...C12	2.802(1)	3.712(5)	154.9(2)	1-x,1/2+y,1-z
	C7-H...C11	2.820(1)	3.739(4)	156.5(2)	1-x,1/2+y,1-z
	C3-H...C13	2.879(1)	3.625(4)	132.8(2)	-x,1/2+y,-z
	C4-H...C14	2.926(1)	3.898(3)	167.3(2)	-x,1/2+y,-z
6	C5-H...O1	2.536(1)	2.941(3)	105.0(1)	1/2+x,-1/2+y,z
	C5-H...C11	2.8013(5)	3.678(2)	150.7(1)	-1+x,y,z
	C4-H...C11	2.8489(4)	3.717(2)	148.1(1)	-1+x,y,z
	C4-H...C11	2.8796(4)	3.735(2)	146.4(1)	x,y,z
	C6-H...O1	2.672(2)	3.487(3)	141.9(1)	1/2+x,1/2-y,-1/2+z
	C1-H...C11	2.9064(5)	3.761(2)	146.2(1)	-1+x,y,z
	C2-H...O2	2.687(2)	3.369(3)	127.0(1)	-1+x,y,z
	C1-H...C11	2.9323(5)	3.824(2)	151.8(1)	-1+x,-y,-1/2+z
7	C2-H...C1	2.6934(3)	3.601(2)	152.7(1)	1/2-x,-1/2+y,1.5-z
	C5-H...C1	2.7132(3)	3.612(2)	152.6(1)	1/2-x,-1/2+y,1.5-z
	C5-H...C1	2.740(1)	3.669(2)	158.5(1)	1/2+x,1/2-y,1/2+z
	C1-H...C1	2.8396(3)	3.746(1)	152.5(1)	1+x,y,z
	C3-H...C1	2.8534(5)	3.701(2)	144.2(1)	1/2+x,1/2-y,1/2+z
	C5-H...O1	2.639(1)	3.077(2)	107.4(1)	-1+x,y,z
7·H₂O	O3-H...C12	2.27(1)	3.075(2)	173(2)	x,y,z
	O4-H...C11	2.35(1)	3.155(2)	173(3)	1+x,y,z
	O4-H...C12	2.46(1)	3.267(2)	170(2)	1-x,1-y,1-z
	O3-H...C11	2.50(1)	3.291(2)	168(2)	1-x,-y,1-z
	C3B-H...O2B	2.515(2)	3.340(3)	140.7(2)	-x,1-y,-z
	C3B-H...C12	2.756(1)	3.616(3)	145.7(2)	x,y,z
	C5A-H...O1B	2.562(2)	3.052(3)	110.9(2)	1-x,-y,-z
	C5B-H...O1A	2.565(2)	3.062(3)	111.4(2)	-x,-y,1-z
	C7B-H...O1B	2.565(2)	3.438(5)	148.4(2)	-1+x,y,z
	C2B-H...C11	2.797(1)	3.709(3)	153.5(2)	-x,-y,1-z
	C2A-H...O2A	2.577(2)	3.377(3)	137.8(2)	1-x,-1-y,1-z
	C3A-H...C11	2.817(1)	3.700(3)	148.9(2)	-x,-y,1-z
	C5A-H...C12	2.819(1)	3.626(3)	140.2(2)	x,-1+y,z
	C5A-H...C11	2.821(1)	3.701(3)	149.8(2)	-x,-y,1-z
	C1A-H...C12	2.840(1)	3.785(3)	160.0(2)	1-x,-y,1-z
C1B-H...C11	2.842(2)	3.702(3)	145.7(2)	x,y,-1+z	
8	C5-H...O6	2.339(3)	3.245(4)	153.3(2)	1+x,1/2-y,1/2+z
	C2-H...O1	2.446(2)	3.389(3)	159.0(2)	-x,-y,2-z
	C3-H...O4	2.463(3)	3.259(4)	137.2(2)	1+x,y,1+z

	C4-H...O3	2.532(3)	3.438(4)	152.0(2)	$x,y,1+z$
	C1-H...O4	2.533(3)	3.372(5)	142.4(2)	$-1-x,-y,1-z$
	C1-H...O5	2.543(2)	3.475(4)	156.8(2)	x,y,z
	C6-H...O3	2.557(3)	3.378(4)	141.4(2)	x,y,z
	C6-H...O6	2.608(3)	3.357(4)	133.3(2)	$1+x,1/2-y,1/2+z$
	C2-H...O5	2.613(3)	3.483(4)	146.8(2)	$-x,-y,1-z$
	C2-H...O2	2.618(2)	3.367(3)	132.5(2)	$-x,-y,1-z$
	C3-H...O6	2.624(3)	3.420(4)	137.4(2)	$1+x,1/2-y,1/2+z$
	C5-H...O4	2.630(3)	3.306(4)	126.3(2)	$1+x,y,1+z$
9	C5-H...O6	2.444(2)	3.358(4)	157.0(2)	x,y,z
	C3-H...O3	2.499(3)	3.471(4)	171.4(2)	$1/2+x,1/2-y,-1/2+z$
	C5-H...O5	2.528(2)	3.482(3)	167.9(2)	$1/2-x,1/2+y,1/2-z$
	C6-H...O6	2.532(2)	3.431(4)	152.4(2)	$-1/2+x,1/2-y,-1/2+z$
	C2-H...O5	2.535(2)	3.453(4)	155.8(2)	x,y,z
	C6-H...O5	2.597(2)	3.388(4)	138.0(2)	$1/2-x,1/2+y,1/2-z$
	C3-H...O4	2.630(3)	3.268(4)	123.0(2)	$1-x,-y,1-z$
	C3-H...O6	2.645(3)	3.517(4)	148.4(2)	x,y,z
	C4-H...O3	2.671(2)	3.397(3)	131.1(2)	$1/2-x,-1/2+y,1/2-z$
	C7-H...O5	2.671(2)	3.517(4)	145.9(2)	$1/2+x,1/2-y,-1/2+z$
10	C4B-H...F4B	2.11(1)	3.09(1)	170.7(3)	x,y,z
	C3B-H...F2B	2.199(8)	3.130(8)	156.0(2)	$1+x,y,z$
	C5B-H...F3B	2.244(8)	3.189(8)	161.3(2)	$1/2+x,1/2-y,-1/2+z$
	C3A-H...F3A	2.391(2)	3.319(3)	155.8(1)	$1.5-x,1/2+y,1.5-z$
	C5B-H...O1A	2.448(2)	3.315(3)	147.2(1)	$1/2+x,1/2-y,-1/2+z$
	C2A-H...F4A	2.399(1)	3.387(2)	175.6(1)	$1.5-x,1/2+y,1.5-z$
	C1A-H...F1B	2.42(1)	3.31(1)	148.2(3)	x,y,z
	C5A-H...F4A	2.440(1)	3.355(3)	155.3(1)	$-1/2+x,1/2-y,-1/2+z$
	C2B-H...F1A	2.459(2)	3.155(3)	127.0(1)	$1-x,-y,1-z$
	C5A-H...F2A	2.461(2)	3.092(3)	121.9(1)	$1/2+x,1/2-y,-1/2+z$
	C5A-H...F3B	2.526(7)	3.392(7)	147.5(2)	$1/2+x,1/2-y,-1/2+z$
	C5A-H...F3A	2.575(2)	3.449(3)	148.6(1)	$1.5-x,1/2+y,1.5-z$
	C4A-H...F2B	2.575(7)	3.181(7)	119.5(2)	$1+x,y,z$
	C6B-H...F4B	2.58(1)	3.45(1)	146.9(3)	$1+x,y,z$
	C2A-H...F4A	2.608(2)	3.446(2)	142.4(1)	$-1/2+x,1/2-y,-1/2+z$
	C1A-H...F3A	2.631(2)	3.036(3)	104.7(1)	$1/2-x,1/2+y,1.5-z$
	C7B-H...F2A	2.631(1)	3.585(3)	164.8(2)	$1+x,y,z$
11	C3-H...N2	2.437(2)	3.304(3)	147.2(1)	$1.5-x,-1/2+y,1/2+z$
	C5-H...N4	2.546(2)	3.375(3)	143.5(1)	$1/2+x,1/2-y,z$
	C2-H...N2	2.559(2)	3.393(3)	142.8(1)	$1.5-x,-1/2+y,1/2+z$
	C7-H...O1	2.584(2)	3.331(3)	133.9(1)	$1.5-x,-1/2+y,-1/2+z$
	C5-H...N2	2.657(2)	3.469(3)	141.5(1)	$1.5-x,-1/2+y,1/2+z$
	C1-H...N2	2.666(2)	3.623(3)	165.5(1)	x,y,z
	C4-H...N4	2.678(2)	3.625(3)	162.6(1)	x,y,z
14	C5-H...F5	2.430(1)	3.395(2)	168.1(1)	$x,y,1+z$
	C5-H...F6	2.473(1)	3.450(3)	174.7(1)	$1/2+x,1.5-y,1/2+z$
	C1-H...F1	2.482(1)	3.446(2)	164.2(1)	$-x,1-y,1-z$
	C5-H...F2	2.493(1)	3.248(2)	133.6(1)	$x,y,1+z$
	C4-H...F4	2.514(1)	3.456(2)	158.8(1)	$1-x,1-y,1-z$

	C2-H...F4	2.523(1)	3.437(2)	153.4(1)	$-1/2+x, 1.5-y, 1/2+z$
	C1-H...F6	2.554(1)	3.391(2)	142.2(1)	$-x, 1-y, 1-z$
	C2-H...F2	2.556(1)	3.452(2)	150.6(1)	$-1/2+x, 1.5-y, 1/2+z$
	C4-H...F6	2.559(1)	3.521(2)	164.0(1)	x, y, z
	C7-H...F3	2.561(1)	3.376(3)	140.6(1)	$1/2-x, 1/2+y, 1/2-z$
	C7-H...F6	2.603(1)	3.507(3)	153.4(1)	x, y, z
	C6-H...F6	2.617(1)	3.330(2)	129.0(1)	$1/2+x, 1.5-y, 1/2+z$
	C4-H...F1	2.643(1)	3.330(2)	126.6(1)	$1-x, 1-y, 1-z$
	C2-H...F3	2.660(1)	3.548(2)	149.5(1)	$x, y, 1+z$
15	C3-H...O5	2.399(2)	3.262(3)	145.3(1)	x, y, z
	C6-H...O5	2.432(2)	3.366(3)	157.2(1)	x, y, z
	C6-H...O1	2.478(2)	3.413(3)	157.2(1)	$x, -1+y, z$
	C5-H...O4	2.508(2)	3.399(3)	151.1(1)	$2-x, 1/2+y, 1/2-z$
	C3-H...O3	2.515(1)	3.333(2)	139.8(1)	x, y, z
	C7-H...O6	2.523(2)	3.469(3)	162.2(2)	$x, 1/2-y, -1/2+z$
	C5-H...O1	2.604(1)	3.263(3)	124.8(1)	$x, -1+y, z$
	C7-H...O6	2.620(2)	3.537(3)	155.9(2)	$1-x, -1/2+y, 1/2-z$
	C5-H...N2	2.677(2)	3.579(3)	153.1(1)	$x, 1/2-y, -1/2+z$
	C1-H...O6	2.648(2)	3.257(3)	119.9(1)	$x, 1.5-y, -1/2+z$
	C3-H...O4	2.697(2)	3.548(3)	144.3(1)	$2-x, 1/2+y, 1/2-z$
	C5-H...O3	2.710(1)	3.532(3)	141.7(1)	x, y, z

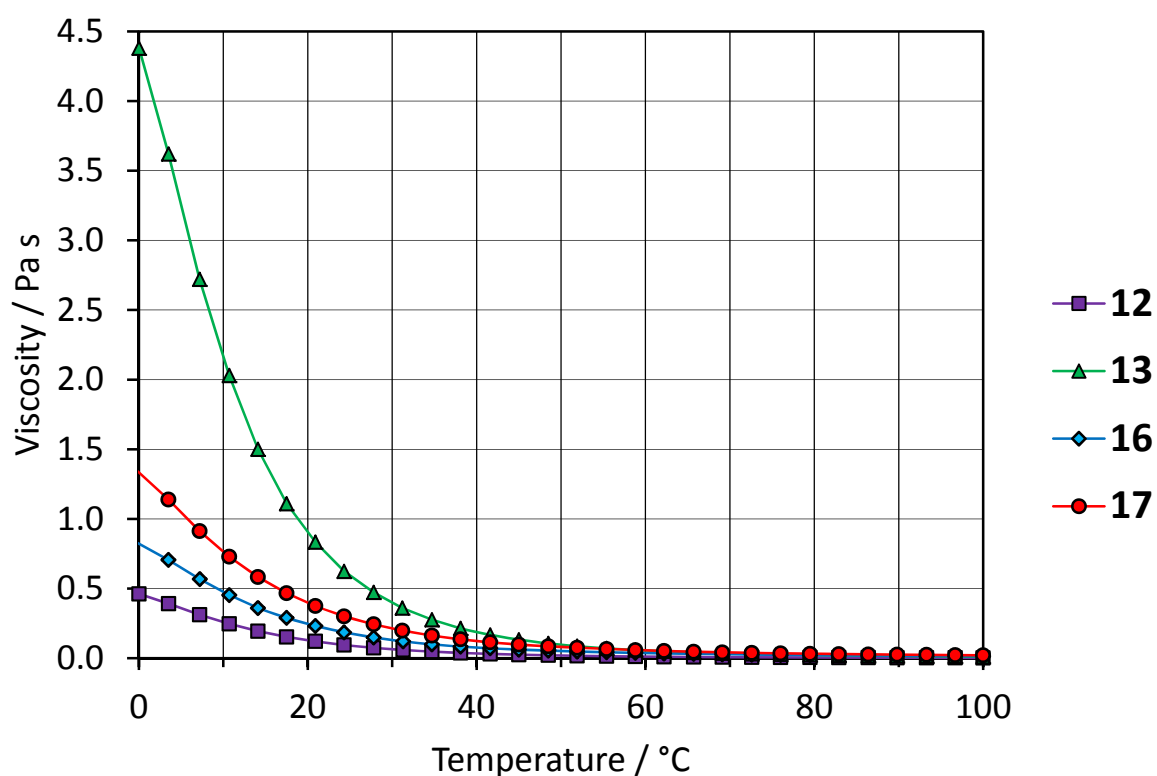


Figure S11. Temperature dependence of dynamic viscosity η of compounds **12**, **13**, **16**, and **17**

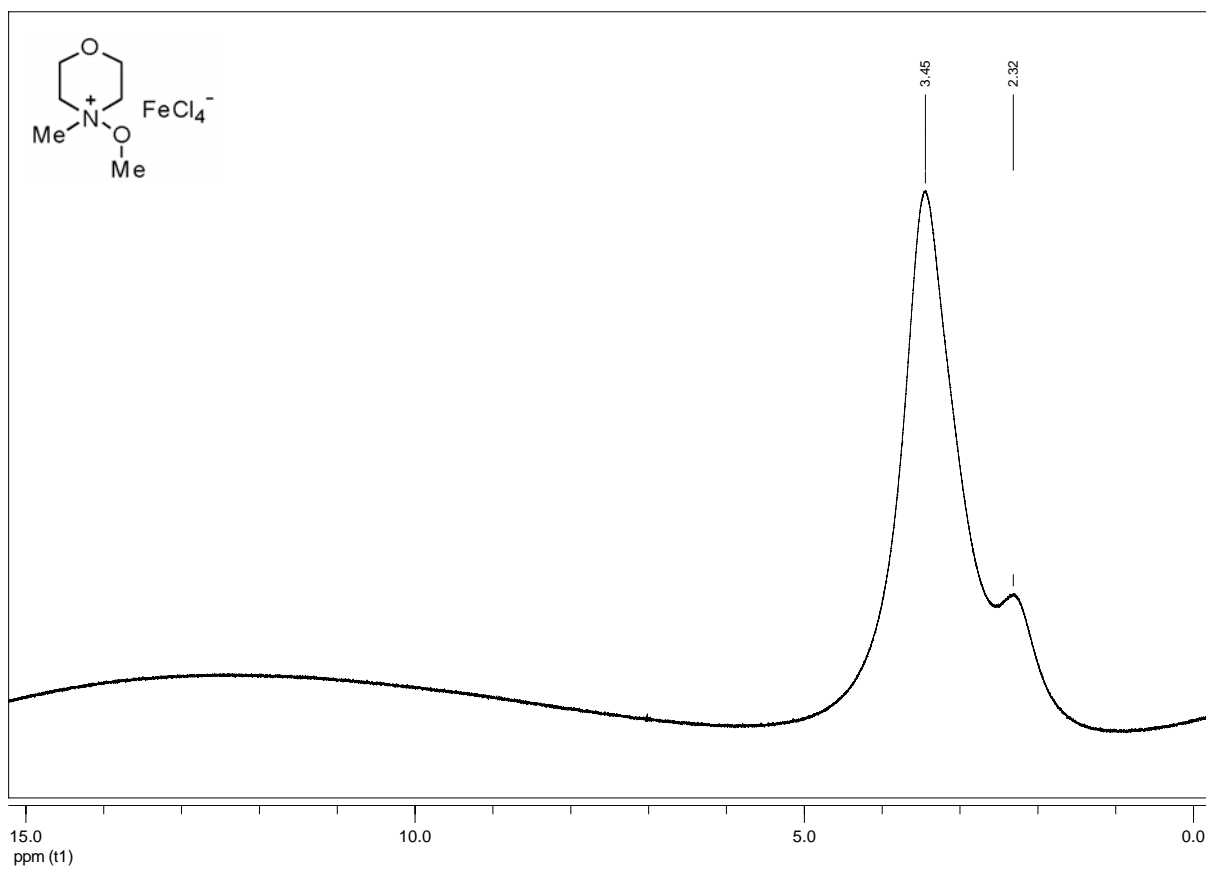


Figure S12. ¹H NMR (300 MHz, DMSO-*d*₆) of *N*-methoxy-*N*-methylmorpholinium tetrachloroferrate(III) (4)

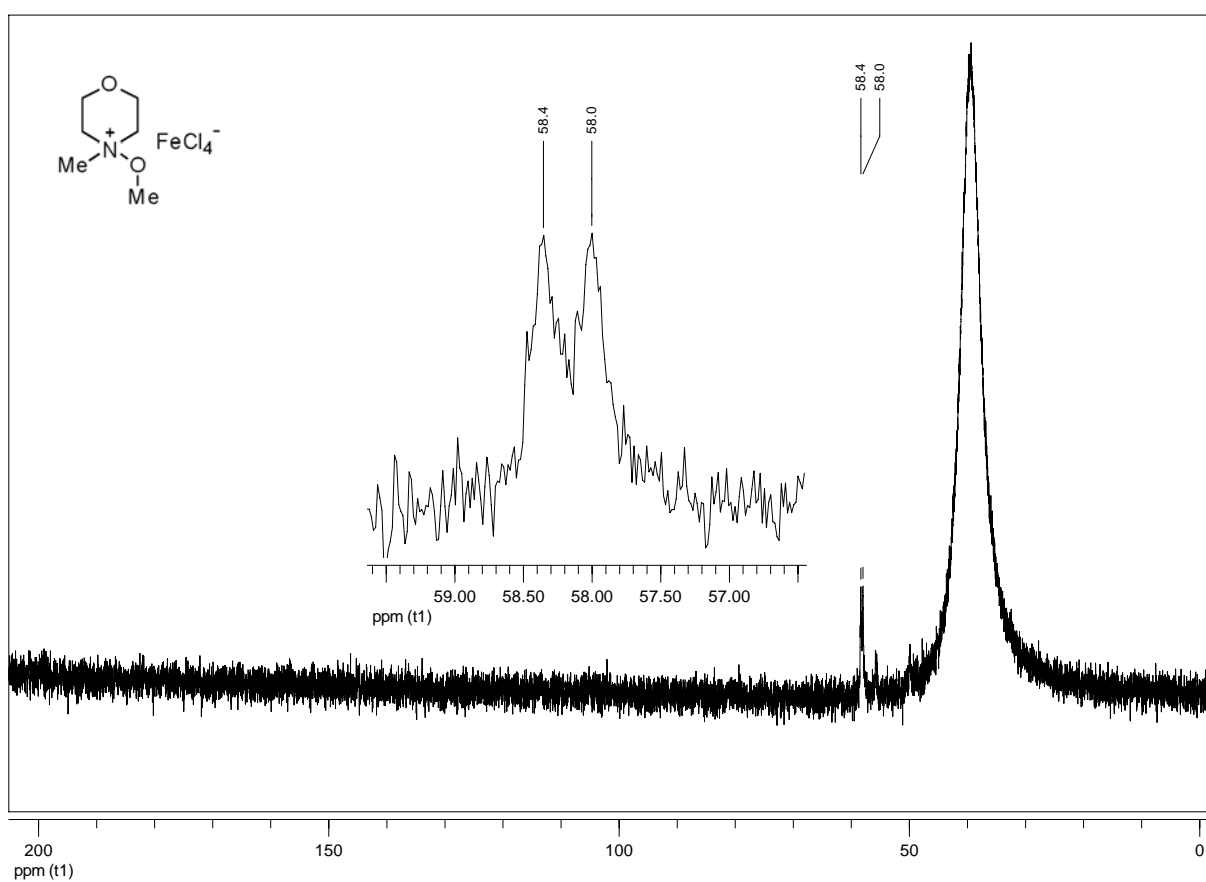


Figure S13. ¹³C NMR (75 MHz, DMSO-*d*₆) of *N*-methoxy-*N*-methylmorpholinium tetrachloroferrate(III) (4)

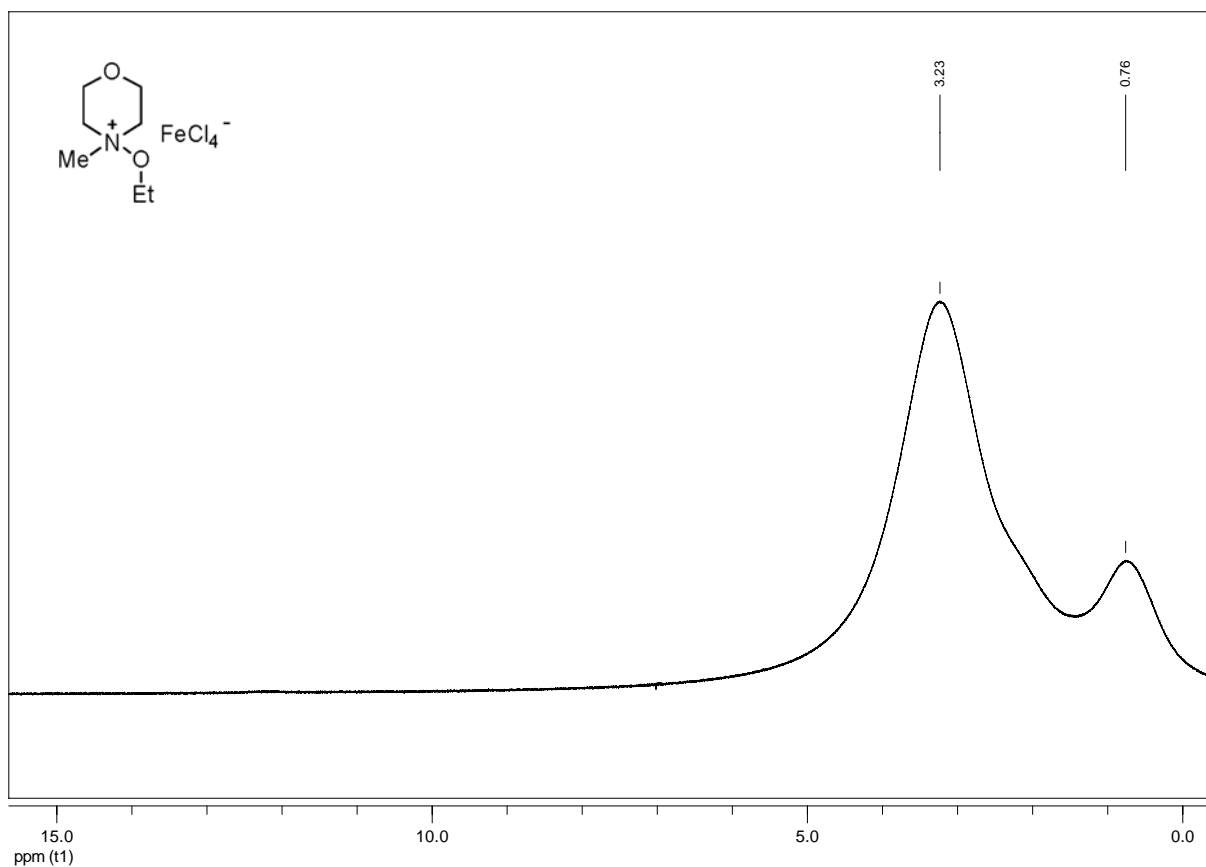


Figure S14. ^1H NMR (300 MHz, $\text{DMSO-}d_6$) of *N*-ethoxy-*N*-methylmorpholinium tetrachloroferrate(III) (**5**)

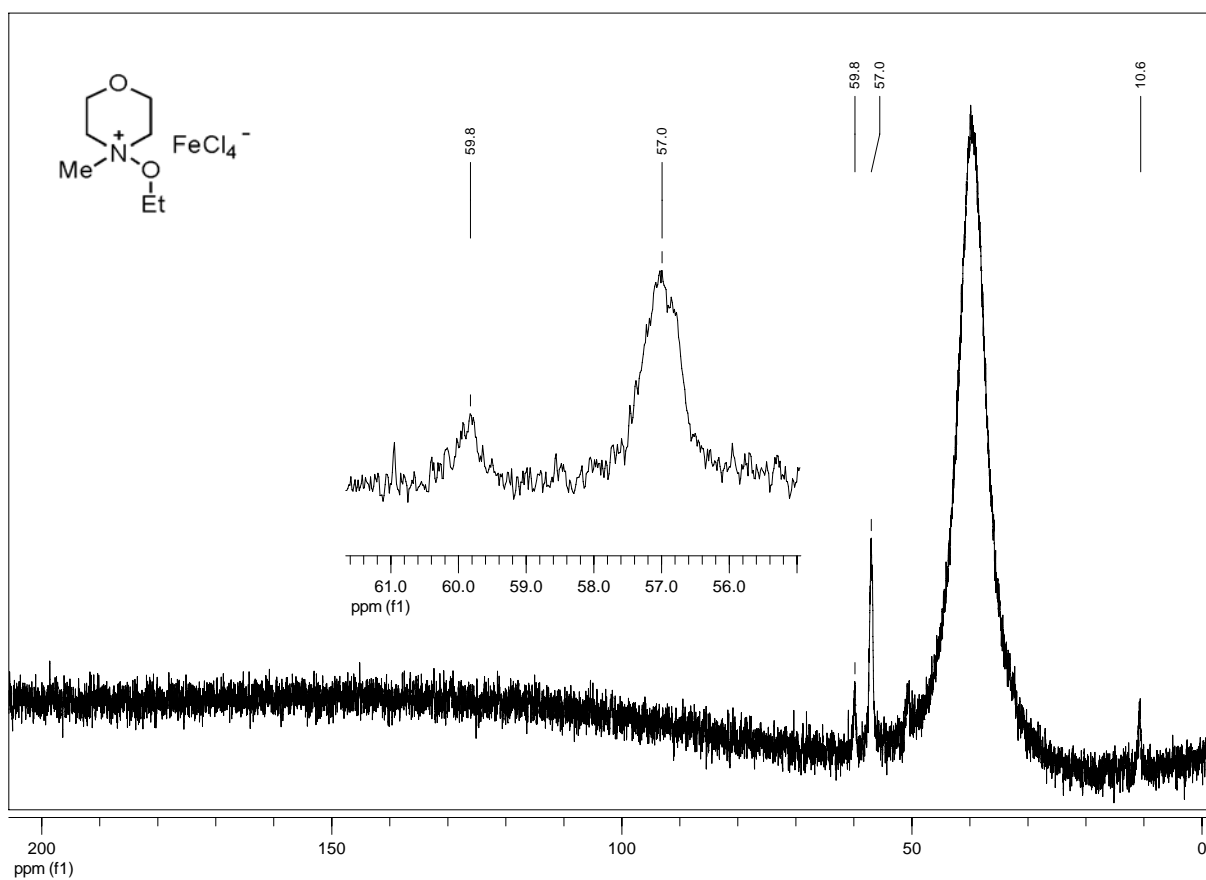


Figure S15. ^{13}C NMR (75 MHz, $\text{DMSO-}d_6$) of *N*-ethoxy-*N*-methylmorpholinium tetrachloroferrate(III) (**5**)

Acetylcholinesterase inhibition assay. The inhibition of AChE was measured using a colorimetric assay based on the reduction of the dye 5,5'-dithiobis(2-nitrobenzoic acid) (DTNB) by the enzymatically formed thiocholine moiety from the AChE substrate acetylthiocholine iodide. The assay has been described in detail.^{S1} Briefly, a dilution series of the test substances in phosphate buffer (0.02 M, pH 8.0) containing max. 1 % MeOH was prepared directly in the wells of a 96-well microtitre plate. DTNB (2 mM, 0.185 mg mL⁻¹ NaHCO₃ in phosphate buffer pH 8.0) and the enzyme (0.2 U mL⁻¹, 0.25 mg mL⁻¹ bovine serum albumin in phosphate buffer pH 8.0) were added to each well. The reaction was started by the addition of acetylthiocholine iodide (2 mM in phosphate buffer). The final test concentrations were 0.5 mM of DTNB and acetylthiocholine iodide and 0.05 U mL⁻¹ AChE respectively. Each plate contained blanks (no enzyme) and controls (no toxicant). Two replicates of nine different concentrations for each substance were tested in each experiment. Two independent experiments with separately prepared stock solutions of each substance were performed. Enzyme kinetics were measured at 405 nm at 30-second intervals in a microplate-reader (MRX Dynatech) for 5 minutes. The enzyme activity was expressed as the slope of optical density (in OD min⁻¹) from a linear regression.

Cell viability assay with IPC-81 cells. Briefly, promyelocytic rat cells from the IPC-81 cell line were incubated with different concentrations of test compounds for 48 h in 96-well plates. Then 2-(4-iodophenyl)-3-(4-nitrophenyl)-5-(2,4-disulfophenyl)-2H-tetrazolium monosodium salt (WST-1) reagent was added and incubated for 4 h. Each plate contained blanks (no cells) and controls (no toxicant). The cell viability assays were generally carried out for a 1:1 dilution series. Each dose-response curve was recorded for 9 parallel dilution series on three different 96-well plates. Two independent experiments with different stock solutions of each compound were performed. Positive controls with Carbendazim were checked in regular intervals.

Reproduction inhibition assay with limnic green algae *Scenedesmus vacuolatus*. For this assay the unicellular limnic green algae *Scenedesmus vacuolatus* (strain 211-15, SAG (Culture Collection of Algae), Universität Göttingen, Göttingen) was used, and toxicity tests were carried out using a synchronized culture. The used test protocol is a modified version of the assay described earlier,^{S2} and the sensitivity is comparable to the standardised 72 h test (ISO 8692). The stock culture was grown under photoautotrophical conditions at 28 °C (± 0.5 °C) in an inorganic, sterilized medium (pH 6.4) containing 8 mM KNO₃, 7 mM NaCl, 2 mM NaH₂PO₄·2H₂O, 1 mM Na₂HPO₄·2H₂O, 1 mM MgSO₄·7H₂O, 0.1 mM CaCl₂·2H₂O, 8 µM H₃BO₃, 2.5 µM MnCl₂·4H₂O, 0.69 µM ZnSO₄·7H₂O, 0.02 µM FeSO₄·7H₂O, 0.02 µM Titriplex III, 0.016 µM (NH₄)₂Mo₇O₂₄·H₂O with saturating white light (intensity of 22 to 33 kilolux) (Lumilux Daylight L 36 W-11 and Lumilux Interna L 36 W-41, Osram,

Berlin, Germany). Cells were aerated with 1.5 vol-% CO₂ and synchronized by using a 14 h light and 10 h darkness cycle. The stock culture was diluted every day to a cell density of 5×10⁵ cells mL⁻¹. The toxicity tests started with autospores (young algal cells at the beginning of the growth cycle). Algae were exposed to the test substances for one growth cycle (24 h). The endpoint of this assay is inhibition of algal reproduction measured as inhibition of population growth. All cell numbers (stock culture and test) were determined with the Coulter Counter Z2 (Beckmann, Nürnberg, Germany). The tests were performed in sterilized glass tubes (20 mL Pyrex tubes sealed with caps containing a gas tight PTFE membrane), algae were stirred over the whole test period of 24 h and the test conditions were the same as for the stock culture except for the CO₂ source. Here 150 µL of NaHCO₃ solution was added to each test tube. The methods for stock culturing and testing have been described in detail previously.^{S3} Laboratory facilities allowed parallel testing of up to 60 tubes. All the substances were tested in three independent experiments. The initial range finding (four concentrations, two replicates) was followed by two additional tests to verify the results with one concentration (1000 mg L⁻¹) per substance in three replicates. The growth inhibition was calculated using the cell counts of the treated samples in relation to the untreated controls (pure medium). For each assay at least 6 controls were used.

Statistical analysis. Statistical analysis was conducted using the software R (version 2.15.1).

Primary biodegradation. The primary biodegradation test was carried out using a modified version of OECD guideline 301 D.^{S4} The concentration of the compound was monitored via ion chromatography (IC) for 28 days. Activated sewage sludge was acquired from the aeration tank of the domestic wastewater treatment plant at Delmenhorst (Germany), the inoculum was filtered and aerated before use. A mineral medium containing final concentrations of 8.5 g L⁻¹ KH₂PO₄, 21.75 mg L⁻¹ K₂HPO₄, 22.13 mg L⁻¹ Na₂HPO₄·2H₂O, 1.7 mg L⁻¹ NH₄Cl, 36.4 mg L⁻¹ CaCl₂·2H₂O, 22.5 mg L⁻¹ MgSO₄·7H₂O and 0.25 mg L⁻¹ FeCl₃ (pH 7.2) was added to the filtrate. In this test a bacteria number of 10⁶ cells L⁻¹ was applied (determined by Paddle-Tester; Hach Europe, Düsseldorf). Samples containing 100–200 µM (ca 60–100 mg L⁻¹) of test substance were prepared, as well as blank samples (inoculated media without test substance), each in replicates. All samples were aerated at 20 °C in the dark during the test. Losses due to evaporation were checked regularly by weighing and balanced by the addition of water. The oxygen content was checked as well. For analysis of the biodegradation 2000 µL of all samples were taken at regular intervals and stored at -18 °C. At the end of the test period the samples were analyzed by IC (Metrohm 881 Compact IC system, equipped with online eluent degasser, 20 µL injection loop and a conductometric detector, maintained at 30 ± 0.1 °C, all Metrohm, Herisau, Switzerland). All chromatographic data were recorded by Metrohm software

MagICNet version 1.1 compact. A silica-based (modified with carboxyl groups) Metrosep C4 ion exchange column (dimensions – 50 × 4.0 mm ID and 5 µm mean particle size) coupled with Metrosep C4 Guard and Metrosep RP Guard was used (all purchased from Metrohm, Herisau, Switzerland). An isocratic method using 40 % acetonitrile in 6 mM nitric acid and a flow rate of 0.9 mL min⁻¹ was applied (limit of detection: <5 µM, limit of quantification: <15 µM). The percentage of biodegradation was determined from the ratio of the peak area to the initial concentration (day 0). Positive controls, imidazole and 1-methyl-3-octylimidazolium chloride, were tested to ensure the general activity of the inoculum.

- S1. F. Stock, J. Hoffmann, J. Ranke, R. Stoermann, B. Ondruschka, and B. Jastorff, *Green Chem.* 2004, **6**, 286.
- S2. R. Altenburger, W. Bödeker, M. Faust, and L. H. Grimme, *Ecotoxicol. Environ. Saf.* 1990, **20**, 98.
- S3. T. Backhaus, M. Scholze, and L. Grimme, *Aquat. Toxicol.* 2000, **49**, 49.
- S4. Test No. 301: Ready Biodegradability, OECD Guidel. Test. Chem. 1992, **301**, 1.